HYDROLOGICAL PROCESSES
Hydrol. Process. **29**, 4932–4946 (2015)
Published online 7 July 2015 in Wiley Online Library
(wileyonlinelibrary.com) DOI: 10.1002/hyp.10551

Energy considerations in groundwater-ridging mechanism of streamflow generation

George W. Waswa[1,2,3]* and Simon A. Lorentz[1,2]
[1] *School of Engineering, University of KwaZulu-Natal, PO Private Bag, X01, 3201, Scottsville, South Africa*
[2] *Centre for Water Resources Research, University of KwaZulu-Natal, PO Private Bag, X01, 3201, Scottsville, South Africa*
[3] *Division of Environmental Mechanics, DPEM, MMUST, PO Box 190-50100, Kakamega, Kenya*

Abstract:

Groundwater ridging is the rapid rise of a shallow water table during a rainfall event, in an environment where, in the pre-event period, the capillary fringe extends to the ground surface. Groundwater ridging is widely cited to account for the observed significant appearance of pre-event water in a stream stormflow hydrograph. Various hypotheses have been advanced to explain the groundwater-ridging mechanism; and most recently, from a field study site in South Africa, an energy hypothesis was proposed, which explains that groundwater-ridging water-table rise is a result of rapid introduction and transmission of additional pressure head into the capillary fringe from an intense rainfall at the ground surface. However, there is a need for further analysis and evidence from other field study sites to confirm and support this newly proposed energy hypothesis. The objectives of this paper are, therefore, as follows: to review previous observations on groundwater ridging, from other study sites, in order to deduce evidence of the newly proposed energy hypothesis; to present and evaluate a one-dimensional diffusion mathematical model that can simulate groundwater-ridging water-table rise, based on the newly proposed energy hypothesis; and to evaluate the importance of a capillary fringe in streamflow generation. Analysis of previous observations from other study sites generally indicated that the rate of groundwater-ridging water-table rise is directly related to the rainfall intensity, hence confirming and agreeing with the newly proposed energy hypothesis. Additionally, theoretical results by the mathematical model agreed fairly well with the field results observed under natural rainfall, confirming that the rapidly rainfall-induced energy is diffusively transmitted downwards through pore water, elevating the pressure head at every depth. The results in this study also support the concept of a three-end-member stream stormflow hydrograph and contribute to the explanation of how catchments can store water for long periods but then release it rapidly during storm events.

KEY WORDS capillary fringe; diffusion mathematical model; potential energy; pressure head; rapid water-table response

Received 25 June 2013; Accepted 21 May 2015

INTRODUCTION

Pre-event water in the stream stormflow hydrograph

Catchment hydrological processes documented in some earlier studies (e.g. Horton, 1933) implied that much of the water in a stream stormflow hydrograph should have a similar isotopic signature as that of the event water, i.e. rainfall. However, with the advent of the use of hydrochemical and isotopic techniques (Craig, 1961), it has been found that pre-event water, which is resident in a catchment before a rainfall event, may appear in significant amounts in a stream stormflow hydrograph (Sklash and Farvolden, 1979).

In most catchments, pre-event water is predominantly groundwater, occurring in the vadose and phreatic zones, and its motion is usually too slow to form a significant fraction of a usually highly transient stream stormflow hydrograph. Among the mechanisms that have been proposed to account for the rapid delivery of pre-event water from catchment soil and geological profiles is the near-stream groundwater ridging (Sklash and Farvolden, 1979; Gillham, 1984; Buttle, 1994).

Groundwater-ridging mechanism

Groundwater ridging is the rapid rise of a shallow water table during a rainfall event, as a result of the rapid *conversion of the capillary fringe*. In this context, a shallow water table is where the tension saturation zone is very close to, or intersects, the ground surface. The conversion process (in groundwater ridging) involves the change in status of the vadose water held in the tension saturation zone (not subject to gravity flow) into phreatic water (subject to gravity flow). The hypotheses that have been proposed to explain the *rapid conversion of the capillary fringe* in groundwater ridging are (1) the

*Correspondence to: George W. Waswa, School of Engineering and Centre for Water Resources Research, University of KwaZulu-Natal, PO Private Bag, X01, 3201, Scottsville, South Africa.
E-mail: waswageorge@gmail.com

fill-meniscus hypothesis and (2) the potential energy hypothesis.

The fill-meniscus hypothesis. The fill-meniscus hypothesis was proposed by Gillham (1984) and supported by Abdul and Gillham (1984), Heliotis and DeWitt (1987) and Novakowski and Gillham (1988). This hypothesis explains that an addition of a very small amount of water at the ground surface fills the capillary meniscus and relieves the capillary tension, resulting in an almost instantaneous rise of the water table to the ground surface. This hypothesis is based on the Young–Laplace equation of capillarity: $h = 2\gamma\cos\theta/\rho gr$, in which h is pressure head, γ is the surface tension of water, θ is the contact angle of the meniscus to the vertical wall, ρ is the density of water, g is the acceleration due to gravity and r is the radius of curvature of the meniscus. Heliotis and DeWitt (1987) explained that by filling the capillary meniscus, the new flat surface meets the vertical wall at an angle of 90° ($\theta = 90°$). This results in $\cos\theta = \cos 90 = 0$, resulting into $h = 0$, interpreted by Heliotis and DeWitt (1987) as the water table having risen to the top of the capillary tube. Here, the top of the capillary tube represents the ground surface in a field situation. This implies that in an environment where the capillary fringe extends to the ground surface, a water table is expected to rise to the ground surface as soon as the capillary meniscus is filled.

Energy hypothesis. More recently, based on field observations from the Weatherley Research Catchment in South Africa, Waswa *et al*. (2013) hypothesized that groundwater-ridging rapid water-table rise is a result of rapid introduction of additional potential energy into the capillary fringe from an intense rainfall at the ground surface. This hypothesis was developed based on the following: (1) field results in which the magnitude of the water-table rise had a direct relationship with the intensity of rainfall; (2) the knowledge that different rainfall intensities are associated with different kinetic energy; and (3) the definition of the tension saturation zone.

In the tension saturation zone, as the name suggests, every pore of the soil is *saturated* (or filled) with water that is entirely dominated by *tension* (negative) energy (Figure 1), because of greater adhesion energy (between the pore water and the solid wall) than the potential/gravitational energy (of the pore water). This implies that the difference between the tension saturation zone and the phreatic zone is in the energy that dominates the pore water; otherwise, both zones are ideally saturated. The pore water in the phreatic zone is dominated by positive (potential) energy (Figure 1); i.e. the potential (gravitational) energy of the pore water is greater than the adhesion energy. The boundary between the two zones is the water table or phreatic surface, along which the pore water is at zero pressure head (i.e. the potential energy of the water is equal to the adhesion energy). In this framework, to convert the vadose water in the tension saturation zone into phreatic water, therefore, requires only an additional energy (i.e. more potential energy to be introduced into the vadose water in the tension saturation zone), without infiltration or additional

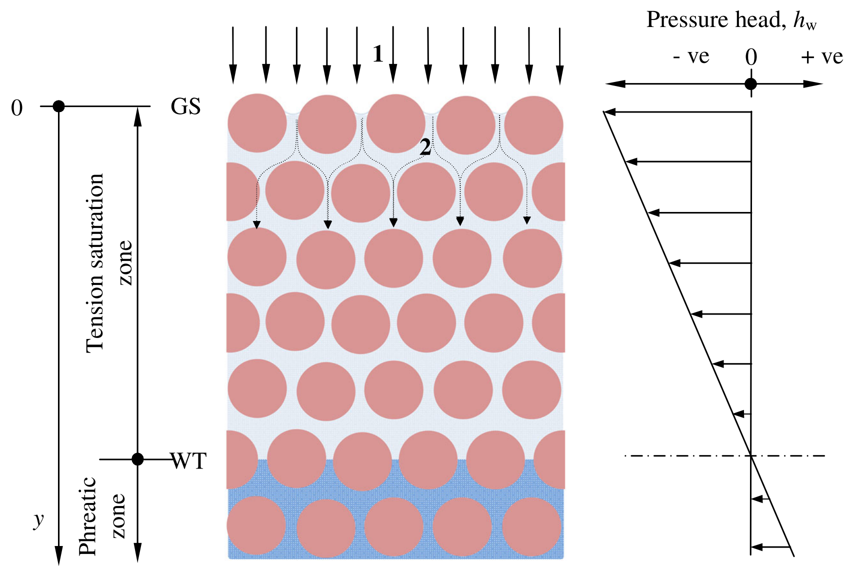

Figure 1. Idealized soil profile with a tension saturated zone extending to the ground surface (GS). Key: *arrow* 1 is intense rainfall that rapidly introduces additional pressure head into the tension saturation zone. *Arrow* 2 is the downward transmission of rainfall-induced pressure head, which rapidly increases the pressure head in the tension saturation zone and elevates the water table (WT). The ground surface is the upper boundary of the capillary fringe, and the water table is the lower boundary of the capillary fringe

water. This additional potential energy raises the total potential energy above the tension (adhesion) energy, converting the vadose water in the tension saturation zone into phreatic water.

There can be various means by which additional energy can be rapidly introduced into the capillary fringe without infiltration, but the most common natural ones are the Lisse effect and groundwater ridging, both of which are described by Waswa *et al*. (2013). In groundwater ridging, the intense rainfall induces a proportionate amount of potential energy into the tension saturation zone, resulting in a proportionate rate and magnitude of a water-table rise. This energy hypothesis was developed based on field observations from a study site in South Africa, and there is a need, therefore, for further analysis and evidence from other field study sites.

The objectives of this paper are, therefore, as follows: (1) to review some of the previous observations on groundwater-ridging mechanism, in order to show the evidence or signals of the energy hypothesis; (2) to present and evaluate a mathematical model that can simulate groundwater-ridging rapid water-table response, based on the newly proposed energy hypothesis; and (3) to evaluate the importance and role of the capillary fringe in streamflow generation.

A REVIEW OF PREVIOUS EXPERIMENTS ON GROUNDWATER RIDGING

Gillham's (1984) field experiment

Gillham (1984) set up a field experiment, in which two tensiometers were installed at different depths in a soil profile. The shallower tensiometer was installed within the capillary fringe and 3 cm below the ground surface. The deeper tensiometer was positioned at the water table, 40 cm vertically below the shallower one. The capillary fringe extended to the ground surface. A 3.8-cm internal diameter water-table observation well was installed in the middle of the site, with the screened interval extending from 30 to 60 cm below ground surface. This implied that of the 43 cm thickness of the capillary fringe, only the lower 13 cm was covered by the screened section of the observation well. The experimental area, 1.5 m in diameter, was levelled, and a low berm was constructed around the perimeter; 0.3 cm of water was *quickly and as evenly as possible* spread on the ground surface, and the reactions of the tensiometers were monitored.

The response of the shallower tensiometer was more rapid and to a higher magnitude (with a change in pressure head of about 30 cm within 15 s) than the response of the deeper tensiometer (with a change in head of 15 cm within 60 s). This difference in pressure-head response generated a hydraulic gradient, which, according to Gillham (1984), indicated downward flow conditions. The piezometer recorded a water level rise of 20 cm (a magnitude that was very close to the response of the deeper tensiometer), but the response lagged behind the tensiometers, which did not also respond instantaneously as had been expected from the theoretical review by the author. This lag in response was attributed partly to non-instantaneous application of water and partly to the compressibility of isolated air bubbles trapped within the soil. Gillham (1984) also observed a flattened peak in the pressure curve of the shallower tensiometer for 15–75 s, during which the free water disappeared from the surface, and the water table remained at 10 cm below the ground surface.

Abdul and Gillham's (1984) laboratory experiments

Abdul and Gillham (1984) used a sand-tank laboratory physical model to investigate the effect of the capillary fringe on streamflow generation and its influence on the groundwater table response to precipitation. The physical model was fitted with an array of tensiometers, which enabled monitoring of pressure-head responses in two dimensions. The model was packed with medium sand, with the surface sloping at 12°. The toe of the slope was fitted with the screened tube to collect free water (streamflow). The sand was slowly saturated from the bottom with de-aired water to eliminate pore air (presumably, having suspected that 'the presence and compressibility of air bubbles' may have been the cause of the observed non-instantaneous response of the tensiometers in the experiment of Gillham, 1984). Five experiments were carried out, with variations in the initial water-table position and the rainfall intensity. Two of these five experiments, namely experiments 1 and 5, had the same initial water-table position, close to the ground surface, and the capillary fringe extended to the entire slope surface. The difference in the two experiments was in the intensity of the applied rainfall: 4.3 cm/h in experiment 1 and 1.9 cm/h in experiment 5. Chloride tracer was added to the simulated rainfall in order to quantify the pre-event and event water in the streamflow discharge. Note that experiment 1 was identical to experiment 4, except for the chloride tracer in the latter.

Results in the transient phase indicated that the shallower tensiometers responded more rapidly than the deeper tensiometers (similar to Gillham, 1984). However, experiment 1 had a shorter transient period (of average 3 min) compared with experiment 5, which had a longer transient period of about 12 min. These researchers also observed lag in response of the tensiometers, contrary to the expected instantaneous responses, and just like Gillham (1984), attributed it to the compressibility of entrapped air within the medium, even after taking precautionary measures to flush out air with de-aired water.

The pre-event water discharge in experiment 1 (of higher intensity rainfall) increased rapidly and to a maximum of 45 cm^3/min (Table I). On the other hand, the pre-event water discharge in experiment 5 (of lower rainfall intensity) increased gradually and to a maximum of 25 cm^3/min. Because the rate of pre-event water (groundwater) discharge was related to the hydraulic gradient, these results indicate that the rate of water-table rise (or response) in experiment 1 (of higher rainfall intensity) was more rapid than in experiment 5 (of lower rainfall intensity) and, hence, agree with the newly proposed energy hypothesis.

Novakowski and Gillham's (1988) field experiments

Novakowski and Gillham (1988) set up their field experiment on an area that consisted of a ridge and a low-lying trough swampy area. The soil profile, in both the ridge and trough areas, consisted mainly of sandy soil. The site was instrumented with 13 tensiometers, within a transect (between the trough area and the ridge area), allowing observations in two dimensions. The initial water table in all the experiments was about 30 cm below ground surface in the trough area and 60–65 cm in the ridge area. Consequently, according to the water retention curve of the soil at this site, the capillary fringe extended to the ground surface in the swampy area but remained at 35 cm below ground surface in the ridge area. Three simulated rainfall events of varying intensities and durations (Table II) were applied, and the responses of the tensiometers monitored.

In the trough area, the water table, which was initially (at the beginning of the rainfall application) at about 30 cm below ground surface, was rapidly elevated by about 15 cm, during the time within which standing water was observed at the ground surface. Shallow tensiometers responded more rapidly and to higher magnitudes than deep tensiometers (similar to Gillham, 1984 and Abdul and Gillham, 1984), resulting in a downward hydraulic gradient. Novakowski and Gillham (1988) reported that even the tensiometers that were well below the water table also responded and that, therefore, the influence of the water-table response may extend to a considerable depth. From the qualitative results reported by Novakowski and Gillham (1988), the rate of the water-table rise in the three experiments was directly related to the rainfall intensity (Table II), being evidence of, and in agreement with, the newly proposed energy hypothesis.

Table II. Rainfall characteristics and the corresponding water-table response observed in the experiments of Novakowski and Gillham (1988)

	Rainfall			Water-table response	
Exp. no.	Duration (min)	Intensity (mm/h)	Total depth (mm)	Rate	Maximum
1	23.35	43	16.7	Fast	Highest
2	5.31	60	5.3	Faster	Higher
3	1.42	63	1.5	Fastest	High

Buttle and Sami's (1992) field observations

Buttle and Sami (1992) carried out a field study on a wetland zone, of which the soil profile was substantially sand, and hence a suitable environment for groundwater ridging. The objective of their study was specifically to carry out a test of the groundwater-ridging hypothesis under field conditions, during snowmelt. They set out to examine whether groundwater ridging, which had been demonstrated for high rainfall intensities, is applicable under snowmelt conditions, when rate of water delivery to the soil surface may be considerably low.

Results indicated that initial melt inputs failed to promote rapid flux of groundwater to the wetland and stream. Instead, Buttle and Sami (1992) observed gradual rise in water levels, following the initiation of surface saturation, contrary to the rapid and pronounced increases observed by Abdul and Gillham (1984).

Summary

A major difference between the experiments of Gillham (1984), Novakowski and Gillham (1988) and Buttle and Sami (1992) is found in the manner in which the water was

Table I. Characteristics of stream flow discharge in response to rainfall events observed during experiments 1/4 and 5 by Abdul and Gillham (1984)

		Average rate of discharge (cm^3/min)/min			Average maximum discharge (cm^3/min)		
	Rainfall intensity (cm/h)	Stream	Pre-event water	Event water	Stream	Pre-event water	Event water
Exp 1/4[a]	4.3	25	15	5	80	45	55
Exp 5	1.9	1	2	0.3	35	25	11

[a] Experiment 1 was identical to experiment 4, except for the chloride tracer in the latter

applied at the ground surface. In the study of Buttle and Sami (1992), water was introduced at the ground surface in a slow manner, i.e. via the *snowmelt*. On the other hand, Gillham (1984) applied the water *quickly and as evenly as possible*. Similarly, Novakowski and Gillham (1988) also applied simulated precipitation of varying *intensity* and duration. It appears, therefore, that the intensity with which water is applied at the ground surface plays a significant role in the rapid rise of a water table in groundwater ridging.

Results and observations from the experimental studies of Gillham (1984), Abdul and Gillham (1984) and Novakowski and Gillham (1988) support and agree with the newly proposed energy hypothesis that the rate and magnitude of the water-table response in groundwater ridging have a direct relationship with the rainfall intensity. The kinetic-energy-laden intense rainfall at the ground surface introduces an additional pressure head (i.e. potential energy per unit weight of water) into the capillary fringe, resulting in groundwater-ridging rapid water-table response, without, or with very little, infiltration. The physical processes of transmission of the rainfall-induced pressure head, rapid conversion of the capillary fringe and the rapid rise of the water table in groundwater ridging are simulated and supported by a mathematical model presented in the following section.

A MATHEMATICAL MODEL FOR TRANSMISSION OF PRESSURE HEAD THROUGH THE TENSION SATURATION ZONE

A differential equation

We consider an idealized capillary fringe as shown in Figure 1. The space coordinate is oriented positive downwards with its origin at the upper boundary of the capillary fringe, which also coincides with the ground surface. The thickness of the capillary fringe is defined by the upper boundary, which is the ground surface, and the lower boundary, which is the water table.

When an intense rainfall occurs at the ground surface, the kinetic energy of the rainfall is imparted into the soil pore water as potential energy and diffusively transmitted downwards. The transmission of the pressure head, h_w, through the pore water can be given by the following equation (Waswa, 2013; Waswa and Lorentz, 2015):

$$\frac{\partial h_w}{\partial t} = d_e \frac{\partial^2 h_w}{\partial y^2} \tag{1}$$

in which t (T) is time, y (L) is depth and d_e $(L^2 T^{-1})$ is the pressure-head diffusivity coefficient and is given as follows:

$$d_e = \frac{\kappa}{\rho_w g} \tag{2}$$

In Equation (2), κ (MT^{-3}) is the pressure-head conductivity of pore water, ρ_w (ML^{-3}) is the density of water and g is the gravitational constant. κ and d_e are analogous to, respectively, hydraulic conductivity and hydraulic diffusivity for transmission/flow of water through porous media and thermal conductivity and thermal diffusivity for conduction of heat through solids.

Initial and boundary conditions

Initial conditions. The assumption here is that at equilibrium, the pressure head below the upper boundary of the capillary fringe increases linearly with depth (Figure 1). To simplify the mathematics and analysis, however, we reduce the initial conditions everywhere to zero, i.e.

$$h_w(y,0) = 0 \quad \text{for}\, y \geq 0 \tag{3}$$

Boundary conditions. The pressure-head conditions at the upper boundary of the capillary fringe are defined and expressed as a function of time as follows:

$$h_w(0,t) = h_w(t)\, \text{for}\, t \geq 0 \tag{4}$$

The conditions at the ground surface will affect, with time, the pressure head at every depth below. This is to say that not only the capillary fringe will be affected but, with time, also the entire depth of the saturated soil profile below the upper boundary of the capillary fringe. This effect was observed and reported by Novakowski and Gillham (1988, p. 29) that 'the influence of the water-table response may extend to considerable depth'. This effect is catered for by the semi-infinite boundary condition:

$$\frac{\mathrm{d}\, h_w}{\mathrm{d}\, y} \to 0, \text{ as } y \to \infty \tag{5}$$

It is important to note here that the change in pressure head at any point within a homogeneous and incompressible fluid depends on the depth of that point relative to some reference plane and is not influenced by the size and shape of the container (Janna, 1983). In other words, the position and the shape of the lower and the side boundaries to the capillary fringe do not have any influence on the change in pressure head at a point within the capillary fringe. More directly, the conditions of the lower and the side boundaries are redundant and would not influence, or be involved in, the analytical solution or observed results.

Solution to the differential equation

The solution to Equation (1), which also satisfies the initial and boundary conditions Equations (3)-(5), takes the following form:

$$h_w(y,t) = h_w(0,t)erfc\left(\frac{y}{\sqrt{4d_e t}}\right) \tag{6}$$

which is analogous to the heat conduction solution (Carslaw and Jaeger, 1959, p. 63).

Estimation of pressure-head diffusivity coefficient

In applying Equation (6), the value of pressure-head diffusivity coefficient (d_e) should be known. Here, this parameter is determined by fitting Equation (6) to the experimental data, in a methodology similar to that employed by Flury and Gimmi (2002), which requires the determination of time to peak, t_p, defined here as the time when the second time derivative of Equation (6) is zero, i.e. $\partial^2 h_w(y, t)/\partial t^2 = 0$, which is

$$t_p = \frac{y^2}{6d_e} \tag{7}$$

By determining t_p for observed data, it is possible to estimate d_e. The theoretical results from Equation (6) are compared with field observations.

FIELD OBSERVATIONS

Study site

The study site is located in the Weatherley research catchment (Figure 2), in the Eastern Cape of South Africa. A detailed description of the entire catchment is found in Lorentz *et al.* (2001) and Waswa *et al.* (2013). The data used in the present study were obtained from the observation point U3 (Figure 2), in the upper subcatchment, within a wetland area and close to a stream, a few metres in the upstream of the upper weir. The vegetation cover at the site was grass that was about a foot tall and with relatively shallow roots. Maximum care was taken to maintain the site in its natural condition.

The soil profile at U3 was relatively uniform. Soil samples from this site were taken to a laboratory for determination of the physical and hydraulic properties, i.e. saturated hydraulic conductivity, soil water retention characteristics and soil particle distribution, of which the values are as indicated in Table III.

Instrumentation

Two ceramic-cup tensiometers, for monitoring pore water pressure responses, were installed in the soil profile at the observation point, as shown in Figure 3. The

Table III. Physical properties of the soils at the observation point U3, sampled from a depth of 0.4 m below ground surface

Quantity	Symbol	Value
Bulk density	ρ_s (kg/m^3)	1818
Porosity	ϕ	0.35
Saturated hydraulic conductivity	K_{sat} (cm/min)	0.19
Pore air entry pressure head	h_b (cm)	45
Pore size distribution index	λ	0.373
Particle size distribution		
Coarse sand (%)		13
Medium sand (%)		16
Fine sand (%)		37
Silt and clay (%)		34

Coarse sand (0.50–2.00 mm), medium sand (0.25–0.50 mm), fine sand (0.053–0.25 mm) and silt and clay (<0.053 mm)

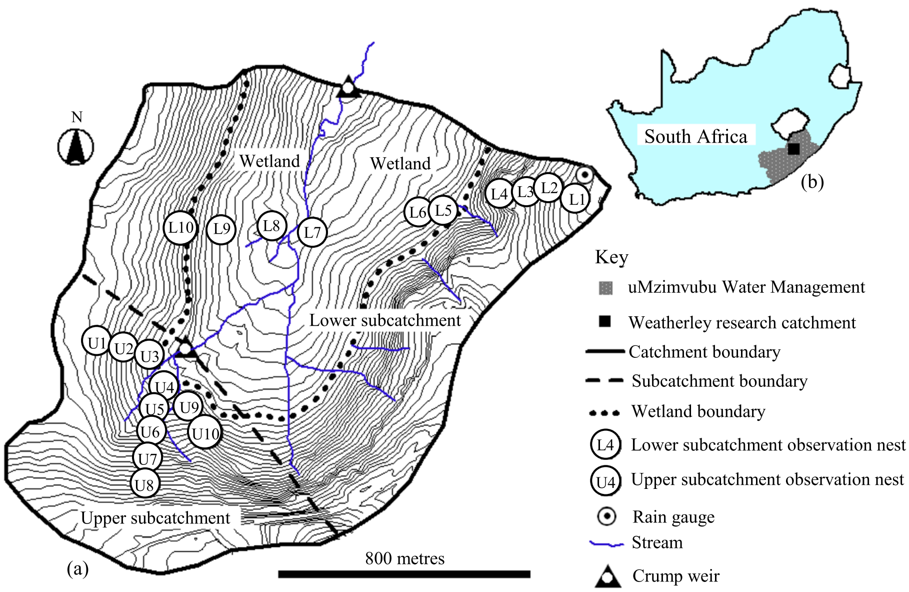

Figure 2. Study site (adopted from Lorentz *et al.*, 2001). (a) The Weatherley research catchment and (b) its location in South Africa

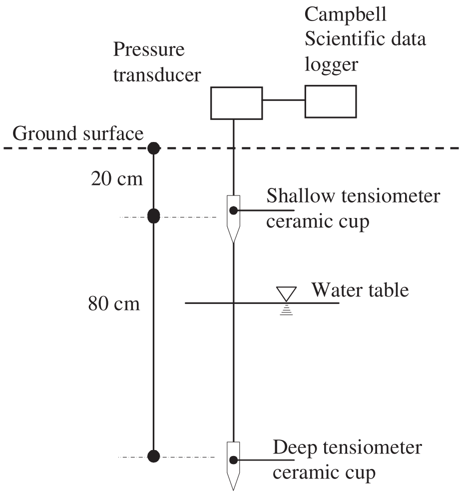

Figure 3. Instrumentation and the positions of the ceramic-cup tensiometers in the soil profile at the observation point U3

shallower tensiometer was installed at 20 cm below the ground surface. The deeper tensiometer was installed at 100 cm below the ground surface and vertically below the upper one. Each tensiometer was connected to a pressure transducer that was then connected to a Campbell Scientific data logger. The pore water pressure-head data were continuously and automatically recorded at 12-min interval and temporarily stored on the data logger before being downloaded to a laptop computer.

Rainfall events

Some of the rainfall events of the summer season of 2000–2001 will be used in this study. Ninety-six rainfall events occurred in that period, of which 11 were found to have caused groundwater-ridging water-table response (Waswa *et al*., 2013; Waswa 2013). In the present paper, we will use six of those events, namely, event nos. 28, 43, 46, 47, 60 and 70.

RESULTS AND DISCUSSION

In all the presented results, the space coordinate is taken oriented positive upwards, with the origin at the upper boundary of the capillary fringe. The energy (pressure head) coordinate is oriented positive downward, with the origin at the water table. For groundwater ridging, the upper boundary of the capillary fringe is at the ground surface.

Observations and conditions for groundwater ridging

It can be noted from Figure 4 that in all the events, the shallow tensiometer responded more rapidly than the deep tensiometer, which responded gradually. From the physical and hydraulic properties of the soil of this site (Table III) and the proximity of the capillary fringe to the ground surface (Table IV), the observed rapid responses are groundwater-ridging phenomenon.

The proximity of the capillary fringe to the ground surface in this study was estimated using two approaches. The first approach is based on the assumption of a linear relationship between pressure head and depth. Noting that the ceramic cup was 20 cm below ground surface and based on the initial values of the pressure head, this first approach yields values of the depths to the water table of between 25.2 and 47.2 cm (Table IV). Consequently, based on this first approach and the pore air entry pressure-head value of the soil (Table III), in all the events, except event 43, the capillary fringe intersected the ground surface. In event 43, the upper boundary of the capillary fringe was about 2 cm below the ground surface, which can be described as very close to the ground surface. The second approach is based on the position of the water table (in the pre-event period) as indicated by the deeper tensiometer. This approach indicates that the water table in the pre-event period in all the six events was between 21.1 and 43.4 cm below ground surface (Table IV). The capillary fringe, therefore, intersected the ground surface in all the events (illustrated in Figure 5a).

In the proposed energy hypothesis, the extension of the capillary fringe to the ground surface is an important condition for groundwater ridging to occur because of two main reasons. First is so that there is a direct and immediate contact between the kinetic-energy-carrying intense raindrops and the potential-energy-deficient pore water. This contact is necessary for rapid transfer of energy from the raindrops to the tension saturation zone. Second is so that there is sufficient and continuous water phase for rapid transmission, to the lower horizons, of the rainfall-induced pressure head (Marui *et al*., 1993). Because the water phase is the medium through which the induced pressure head is transmitted, groundwater ridging is commonly observed in areas with coarse-textured (sandy aquifers) soils and hardly observed in areas with fine-textured soils. This is because, coarse soils contain large and less tortuous pores, and hence, when filled with water, they provide an ideal condition (pathways) for rapid transmission of the induced pressure head. This was evident in separate laboratory experiments on the Lisse effect (Waswa and Lorentz, 2015), which showed more rapid transmission of pressure head through pore water in coarse-textured soil than in fine-textured soils. This explains why high rainfall intensities on fine-textured soils cannot generate or result in groundwater-ridging rapid water-table response, contrary to the expectations of Gillham (1984, p. 314) that 'for fine textured materials, even larger responses could be expected'. These conditions, necessary for groundwater-ridging rapid water-table response, have also been outlined by

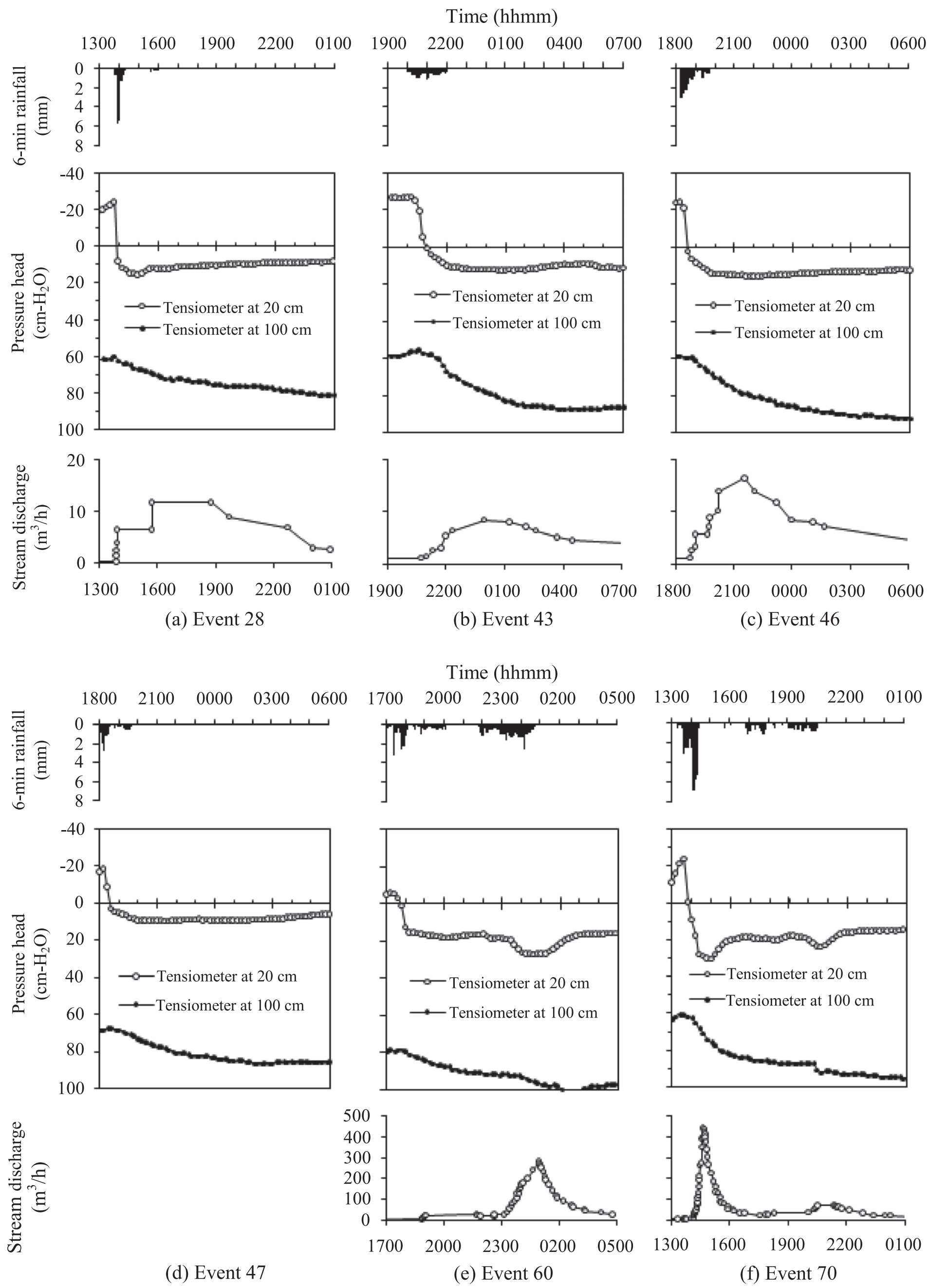

Figure 4. Pressure-head responses at U3 and stream discharge over the upper weir

Cloke *et al*. (2006, Table 1), as the 'riparian characteristics and evidence for groundwater ridging mechanism'.

Pressure head and water-table response behaviour

The rate of pressure-head decline in the shallow tensiometer in all the rainfall events was nearly the same, but not rapid (Figure 4), contrary to the observations from field experiments of Gillham (1984) and Novakowski and Gillham (1988). This contradiction indicates that the rate of decline of the pressure head, after its rapid elevation in the capillary fringe, is not an intrinsic characteristic of groundwater ridging, as implied by Heliotis and DeWitt (1987) and Miyazaki *et al*. (2012). Instead, the rate of decline depends on the environmental conditions and the design and settings of the monitoring system. For instance, the experimental designs of Gillham (1984) and Novakowski and Gillham (1988) were such that the additional energy from the intense rainfall was introduced into the capillary fringe through small surface areas, around the monitoring points or probes. This

Table IV. Depth from ground surface to the water table (thickness of the capillary fringe) in the pre-event period

Rainfall				Tensiometer at 20 cm		Tensiometer at 100 cm	Depth (cm) to water table based on the following	
Event no.	Date	Total depth (mm)	Max 6-min r/fall (mm)	Start PH (cm H_2O)	Max PH (cm H_2O)	Pre-event PH (cm H_2O)	PH–D relationship	Deep tensiometer (at 100 cm)
28	28.11.00	16	5.8	−23.9	15.7	59.6	43.9	40.3
43	08.01.01	20	1.2	−27.2	12.6	56.6	47.2	43.4
46	13.01.01	28	3.0	−24.4	16.0	58.5	44.4	41.5
47	18.01.01	11	2.8	−18.3	9.8	68.6	38.3	31.4
60	13.02.01	56	3.2	−5.2	18.5	78.9	25.2	21.1
70	10.03.01	47	6.8	−23.6	30.4	60.8	43.6	39.2

PH, pressure head; D, depth; r/fall, rainfall

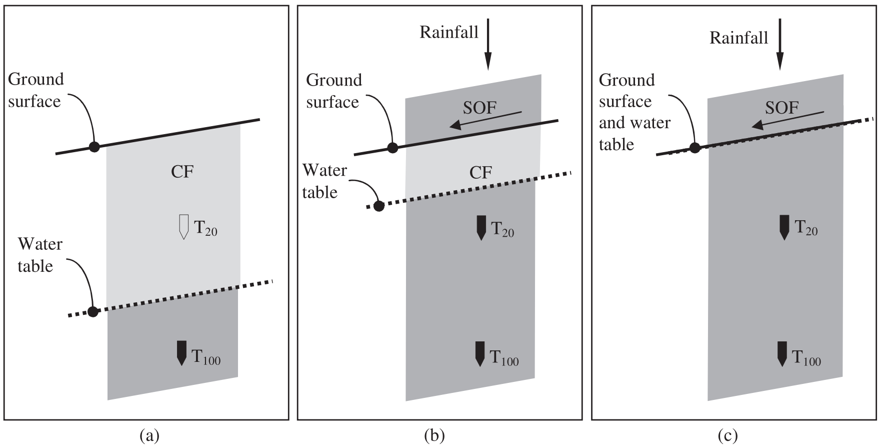

Figure 5. (a) The initial (pre-event) conditions with a capillary fringe extending to the ground surface; (b) only a fraction depth of the capillary fringe is converted (e.g. events 28, 43, 46, 47 and 60); (c) the entire capillary fringe is converted, resulting in a continuous water phase of positive pressure head (e.g. event 70). CF is capillary fringe, SOF is saturated overland flow, T_{20} is tensiometer at 20 cm below ground surface and T_{100} is the tensiometer at 100 cm below ground surface

resulted in the formation of a small water-table mound (Marino, 1974) within a large domain of the capillary fringe, which also resulted in a rapid dissipation (through drainage) of the injected energy and hence a rapid decline in the pressure head. However, if the ground surface area over which the energy is injected is large (as expected under natural rainfall) and if the monitoring point/probe is at the middle of the area, the water table would rapidly rise over the entire area, but the rate of decline of the pressure head would not be rapid.

Because the position of the shallower tensiometer was known (20 cm below ground surface), it is possible to estimate the transient position of a water table during the events, based on the pressure-head values indicated by this tensiometer. For instance, when the shallower tensiometer indicated zero pressure head (0 cm H_2O), it implied that the water table was at the position of the ceramic cup of the tensiometer (20 cm below ground surface). When the tensiometer recorded a pressure-head value of 20 cm H_2O, it indicated that the water table was at the ground surface. Based on this approach, it can be seen from Table IV and Figure 4 that the water table was elevated to different depths in different rainfall events. In some events, e.g. event 43, the water table remained below the ground surface (maximum pressure head of less than 20 cm H_2O), as illustrated in Figure 5b. In other events, e.g. event 70, the water table seemed to have been elevated above the ground surface. Event 70 had the highest 6-min rainfall intensity (6.8 mm) that introduced into the capillary fringe a proportionately high amount of energy, more than what was required to just elevate the water table to the ground surface. This entire conversion of the capillary fringe resulted in a continuous water phase under positive pressure head, including the saturated overland flow that rapidly developed at the ground surface, as soon as the rainfall started.

Overland flow over a capillary fringe

During the rainfall events, in which the water table did not reach the ground surface, the overland flow may have formed over a tension saturated soil profile, as illustrated in Figures 5b and 9. This process may result in three horizons of water: (1) the saturated overland flow, or free-standing water (under positive pressure head) above the ground surface; (2) the unconverted depth of the tension saturation zone, immediately below the ground surface; and (3) the phreatic zone below the water table (Figure 5b). This discussion on the overland flow over a tension saturation zone is supported by comparing the temporal evolution of the stream discharge over the upper weir *vis-à-vis* the rise in a water table at the nearby observation point U3 (Figure 6). We note that in all the events, the stream discharge significantly increased before, or even without, the arrival of the water table at the ground surface. For instance, in event 70 (Figure 6d), when the water table was at 20 cm below the ground surface at U3, the stream discharge had increased from 1 to 5 m^3/h. In other events (e.g. event 28, event 43 and event 46), the stream stormflow hydrograph (discharge) rose to peak and declined, while the water table at U3

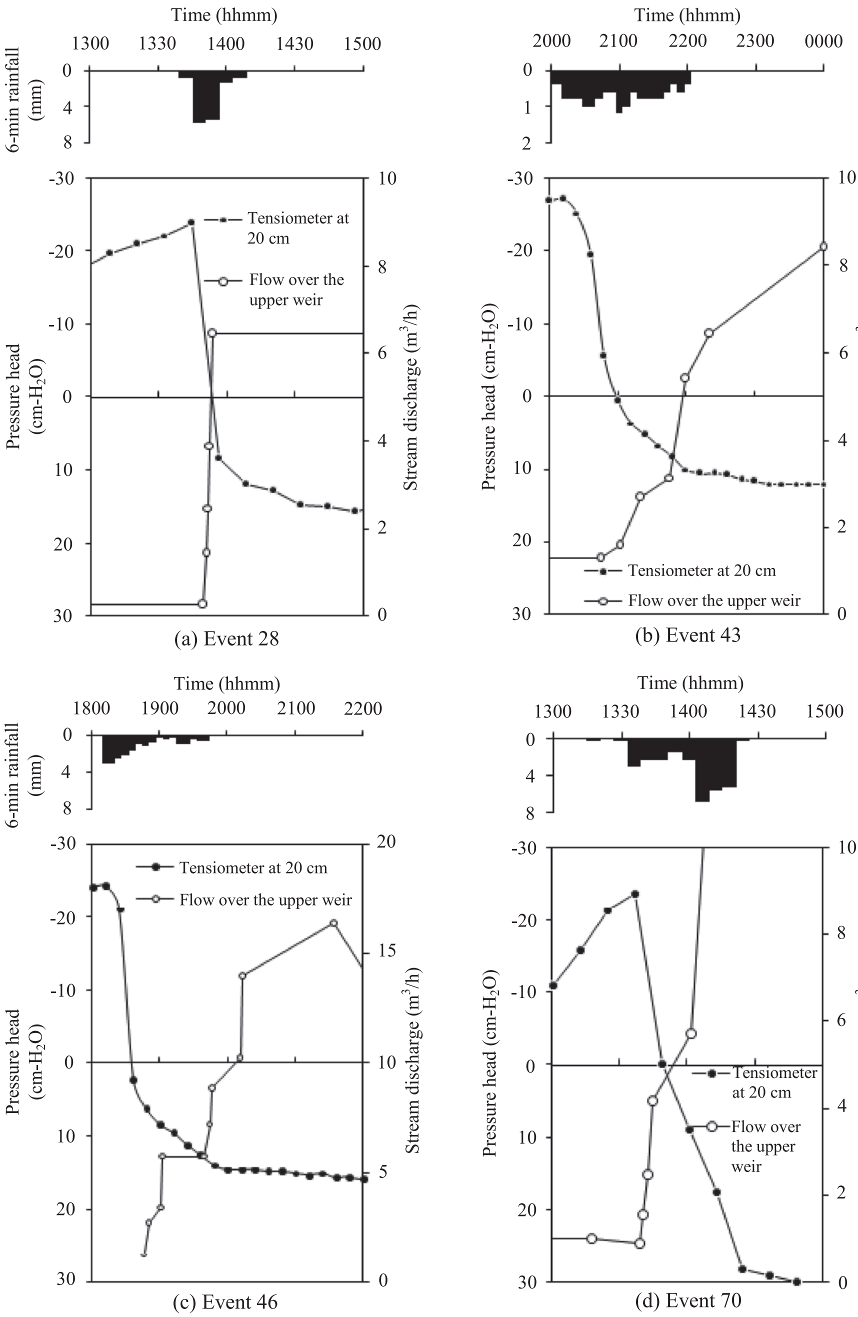

Figure 6. Time comparison of stream discharge over the upper weir and pressure-head responses at U3, demonstrating that overland flow might have occurred over a tension saturated soil profile

remained below the ground surface. For instance, in event 43 (Figure 6b), the stream stormflow hydrograph increased to a maximum of 8 m^3/h and recessed, while the water table at U3 remained at about 8 cm below the ground surface. Similar observations of free water over a tension saturated soil profile have been reported before. Gillham (1984: pp. 316 and 317) reported of free water at the ground surface, while the water table was still rising, and of which the maximum rise was 10 cm below the ground surface. Novakowski and Gillham (1988) also observed free-standing water in the trough area before the end of the rainfall application period, within which the water table was elevated to only 15 cm below the ground surface. It is important to note here that a depth (pressure head) of free water at the ground surface is also transmitted through a capillary fringe, resulting in an equivalent rise of a water table. For instance, an overland flow, or ponded water, of 10 cm will result in the rise of a water table by 10 cm. This is in addition to the pressure head introduced by the kinetic energy of the raindrops. This explains the observations made by Novakowski and Gillham (1988), in which the rate of response of the water table was directly related to the rainfall intensity, but the maximum rise of the water table was directly related to the rainfall amount (Table II).

Transmission of pressure head through capillary fringe

Field observations. A correspondence can be noted between the responses of the tensiometers at U3 (Figure 4). The response of the shallower tensiometer is immediate and almost matching the pattern of the rainfall event at the ground surface. The response of the deeper tensiometer is relatively delayed, attenuated and considerably muted, with respect to the rainfall pattern. However, it is clear that the two tensiometers responded to the signals generated by the rainfall events at the ground surface, with the responses being translated in time and the magnitude being attenuated with depth (similar to a flood wave between two points along a stream). These field observations are used to evaluate the presented mathematical model.

Comparison of field observations and theoretical results. To use Equation (6) to predict pressure head, we require the value of pressure-head diffusivity (d_e) and the ground surface pressure-head conditions (Equation (4)). Pressure-head diffusivity coefficient was estimated using Equation (7) and the observed pressure-head data at the deeper tensiometer. d_e of 31 cm^2/min was obtained. Because we did not monitor pressure head at the ground surface, we adopt the position of the shallower tensiometer as our upper boundary. The section under consideration, therefore, is the 80-cm-thick saturated soil profile between the two observation points: the shallower position (20 cm below ground surface) as the upper boundary of the section and the deeper position (100 cm below ground surface) as the prediction point.

The theoretical results (by Equation (6)) and observed field results for 6 h (240 min) are as shown in Figure 7. It can be seen that the mathematical model predicted, with good accuracy, the observed pressure head at the prediction point. While the pressure head at 20 cm below ground surface increases instantaneously and rapidly, both the theoretical (predicted) and observed results at 100 cm below ground surface indicated a delayed and gradual increase in pressure head. Similar observations of delayed responses in tensiometers were reported by Gillham (1984), Abdul and Gillham (1984), and Novakowski and Gillham (1988) and attributed to the presence and compression of entrapped pore air. On the contrary, both the theoretical and field observed results presented here indicate that the delayed responses are a result of the time required for the energy to be transmitted from the source (ground surface) to the regions below.

The transmission of energy through the saturated soil profile can also be inferred from the vertical orientation patterns of the pressure lines at different times (Figure 8). In the pre-event period (0 h), the gradients of the pressure lines were approximately -1. One hour after the onset of the rainfall event, pressure head at the shallower tensiometer had been elevated to about six times the pressure head at the deeper tensiometer, significantly altering the pressure gradient from the pre-event conditions. Twelve hours after the onset of the rainfall events, the pressure-head lines are again indicating a new equilibrium, with the gradients close to -1. However, this new equilibrium is at an elevated state of energy, as indicated by the elevated water-table positions. These vertical orientations of the pressure lines indicate the direction of transmission of pressure head, as well as the elevation of energy at different depths and times. At the onset of a rainfall event, the pressure head is rapidly introduced into the system via the upper boundary of the capillary fringe, which coincides with the ground surface. The introduced pressure head is transmitted downwards, resulting in a corresponding increase in pressure head at every depth below the ground surface (including the capillary fringe and the phreatic zone), and hence the rapid rise in the water table. Ultimately, every depth of the soil profile below the ground surface achieves a new equilibrium at an elevated state of energy. These adjustments in pressure heads result in adjustments in hydraulic heads (gradients), which in turn result in adjustments in water flow. It is worth mentioning that the geometrical configurations of the pressure lines at 0

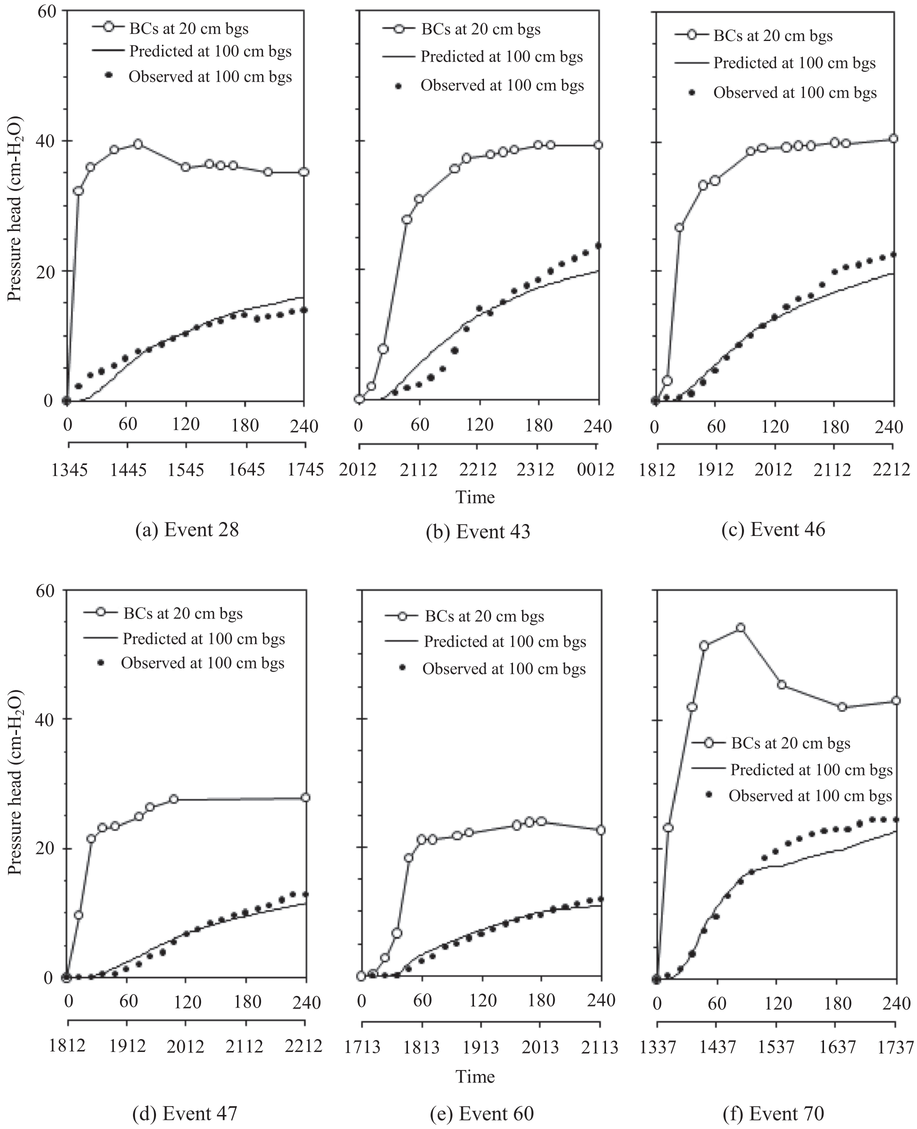

Figure 7. Observed *versus* predicted (by Equation (6)) pressure-head responses at 100 cm below ground surface (bgs) at the observation point U3. On the time (x) axis, the upper values are relative time from the start of response of the shallower tensiometer, and the lower values are the absolute clock time. BCs is boundary conditions, and bgs is below ground surface

and 1 h (Figure 8) are in agreement with Equation (5): the change in pressure head per the change in depth tends towards zero (becomes negligible) as the depth from the energy source becomes large.

Effect of groundwater ridging on groundwater flow patterns

Groundwater flow patterns at the wetland zone in the study catchment can be inferred from a comparison of the responses at two adjacent monitoring points, i.e. U3 and U2. Comparing the responses of the tensiometers in event 43, indicates that the water-table rise at U3 was more rapid and to a higher magnitude than that at U2 (Figure 9). These disproportionate responses in the water table may have had significant changes on the horizontal hydraulic gradient and, hence, on the local groundwater flow patterns in the wetland area. Similar observations were also made by Rosenberry and Winter (1997) and Novakowski and Gillham (1988). These results demonstrate that the water table in wetland areas can be very dynamic and that in areas of irregular topography, the complex change in water-table elevation can result in highly complex and transient groundwater flow patterns.

Role of capillary fringe in streamflow generation

The results reported in this study demonstrate the various roles of the capillary fringe in streamflow generation. First,

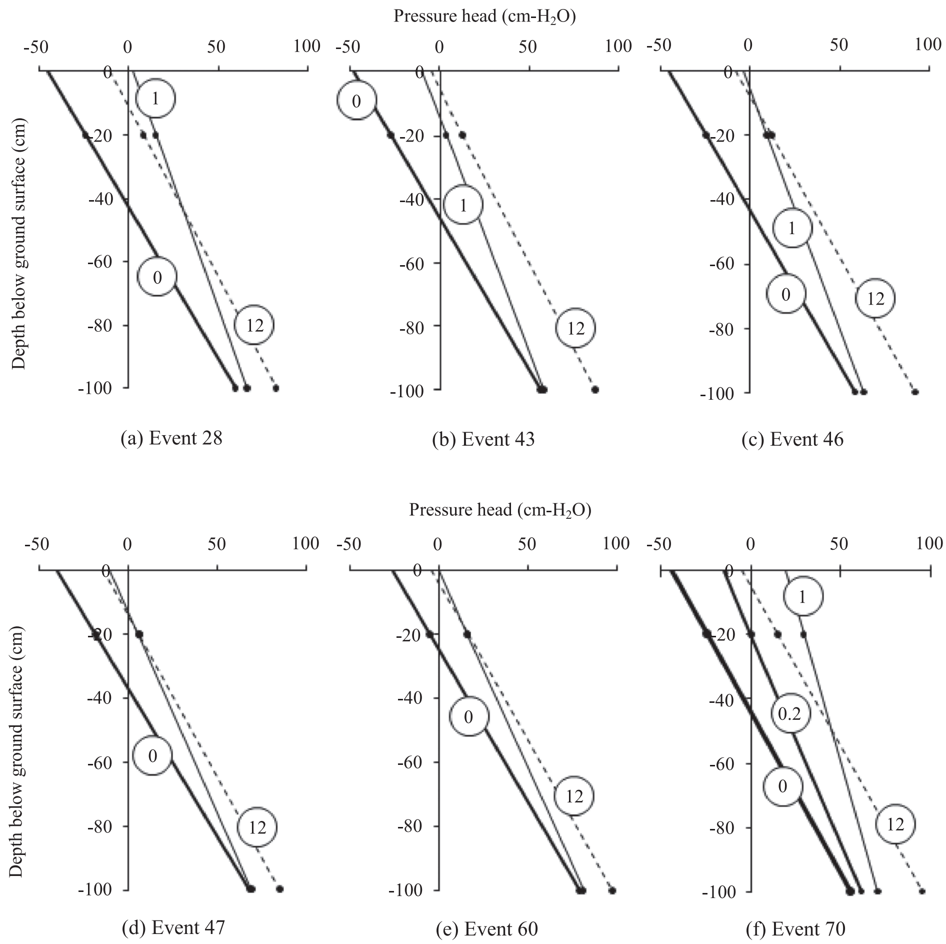

Figure 8. Vertical profiles of pressure head at the observation point U3 at 0, 1 and 12 h after start of the response of the shallower tensiometer

the close proximity of the capillary fringe to the ground surface minimizes or eliminates the possibilities of rainfall infiltration at the ground surface. This means an immediate formation of saturated overland flow at the onset of a rainfall event, hence faster and greater delivery of rainwater (event water) to a nearby stream. Second, the rapidly converted capillary fringe (from tension-dominated/tension-held water to phreatic water) allows the pre-event water stored in the capillary fringe to be mobilized by gravity to a nearby stream, via either expanded seepage face (Figure 9) or steepened lateral hydraulic gradient or both (Abdul and Gillham, 1984; Cloke *et al*., 2006).

The roles of the capillary fringe and the energy hypothesis presented here support the concept of a three-end-member stream stormflow hydrograph and might provide an explanation to 'how catchments can store water for long periods, but then release it rapidly during storm events, and vary its chemistry according to the flow regime' (Kirchner, 2003). The water in the vadose zone, which includes the capillary fringe, has been found to be isotopically heavier than phreatic zone water (Buttle, 1994), partly as a result of enrichment by evaporation of water from the vadose zone. The rapid conversion of the capillary fringe water to phreatic water enables this isotopically heavier water to be rapidly delivered, by gravity flow, into a nearby stream. The rapid arrival of the enhanced and isotopically heavier water from the capillary fringe (arrow 5 in Figure 9) into the stream, in addition to the much heavier event water (from the rainfall), results into a two-end-member hydrograph. But note that the introduced additional energy diffuses downwards even into the phreatic zone (as also observed and reported by Novakowski and Gillham, 1988), raising its pressure head. The increase in energy content of the pre-event phreatic water increases its mobility, out of the soil profile, compared with the pre-event period (arrow 7 in Figure 9). This results in the reported three-end-member stream stormflow hydrograph, consisting of (1) event water; (2) pre-event capillary fringe water or, generally, the vadose zone water; and (3) pre-event phreatic water (Kennedy *et al*., 1986; Dewalle *et al*., 1988; Swistock *et al*., 1989; Ogunkoya and Jenkins, 1993).

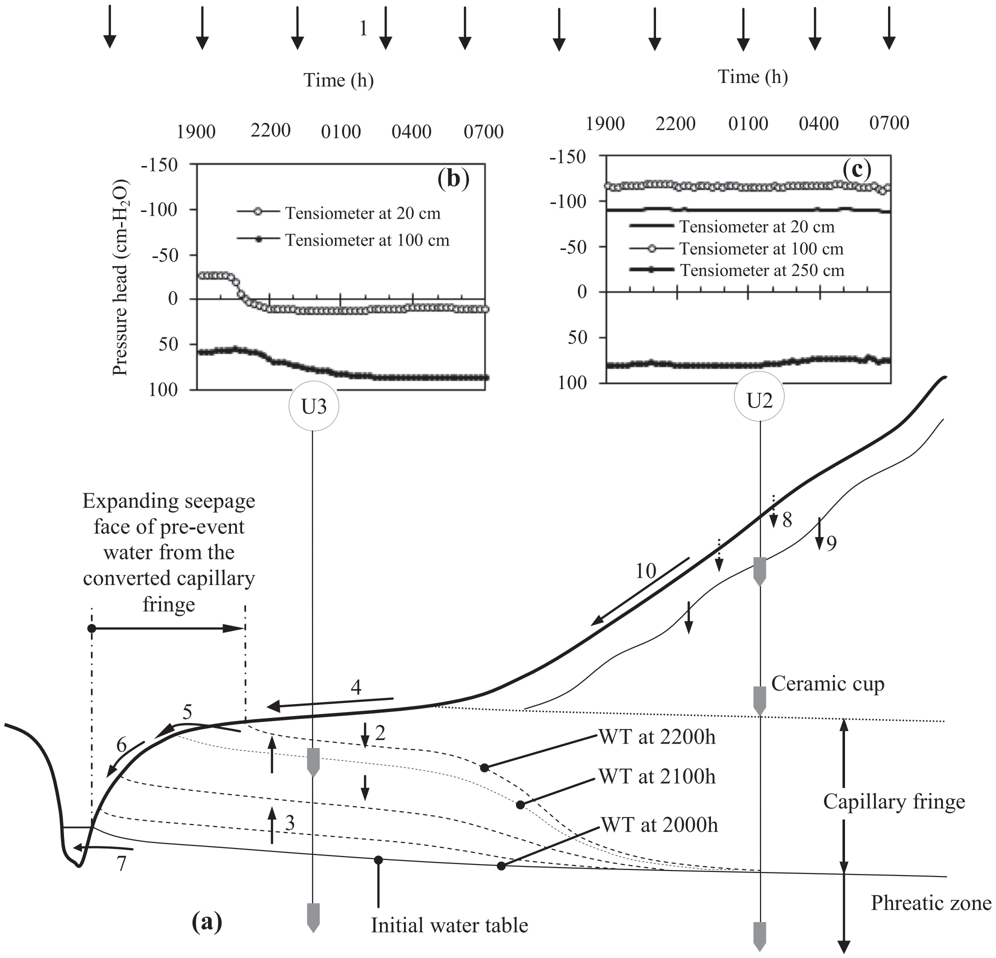

Figure 9. (a) Illustration of local groundwater table responses between observation points U3 and U2 (see Figure 2 for their spatial positions) and from the responses of the tensiometers at (b) U3 and (c) U2, during event 43. *Key to arrows*: 1, intense rainfall (pattern shown in Figure 4b); 2, transmission of rainfall-induced pressure head; 3, rising water table (locus of zero pressure head); 4, saturation overland flow (over the capillary fringe), mainly event water; 5, seepage of pre-event water from the converted section of the capillary fringe; 6, saturation overland flow (a mixture of pre-event water from capillary fringe and event water); 7, enhanced seepage of pre-event phreatic water (baseflow), as a result of increased energy; 8, infiltration of rain water; 9, infiltration profile through unsaturated zone; and 10, Hortonian overland flow

CONCLUSION

The recently proposed energy hypothesis has been applied to explain the rapid water-table rise in groundwater ridging. This application is based on the understanding that the only difference between the vadose water in the tension saturation zone and the phreatic water is in the type of energy that dominates the water; otherwise, both zones are saturated and cannot absorb more water in the form of infiltration. The vadose water in the tension saturation zone is dominated by tension energy, as a result of greater adhesion energy (between the pore water and the solid wall), than the potential/gravitational energy of the water. The dominance of the tension energy decreases with depth as the gravitational energy increases, and at the water table, where the two forces are equal, the pressure head is zero. Below the water table, the gravitational energy dominates the pore water. During a rainfall event and where the zone of tension saturation extends to the ground surface, the kinetic energy of the rainfall is rapidly imparted into the vadose water in the tension saturation zone, as an additional potential energy, rapidly converting it into phreatic water.

A review of literature has shown that the proposed energy hypothesis is also evident in the results reported in previous experimental field and laboratory studies on groundwater ridging (e.g. Gillham, 1984; Abdul and Gillham, 1984; Novakowski and Gillham, 1988). Generally, these previous results indicate that the rate of the water-table rise in groundwater ridging is directly related to the intensity of rainfall at the ground surface.

The additional rainfall-induced pressure head is rapidly and diffusively transmitted through pore water, raising the pressure head at every depth of the saturated soil profile (including the capillary fringe and the phreatic zone). These processes are supported and verified by a one-dimensional mathematical diffusion model, from which the theoretical results were in good agreement with the observed results from field observations obtained under natural rainfall.

The newly proposed energy concept supports the hypothesis of a three-end-member stream stormflow hydrograph, consisting of event water, pre-event vadose water and pre-event phreatic water. This proposed energy hypothesis, consequently, also provides a physical explanation of 'how catchments can store water for long periods, but then release it rapidly during storm events, and vary its chemistry according to the flow regime' (Kirchner, 2003).

However, further studies are recommended to confirm the proposed energy concept. Well-designed and instrumented field studies and laboratory experiments (using sand-tank models, such as that employed by Abdul and Gilham, 1984, and sand column experiments) should be carried out to specifically evaluate the newly proposed energy hypothesis of the groundwater-ridging water-table response. These recommended further studies should also incorporate hydrochemical observations to clearly verify the role of the proposed energy hypothesis in the conversion of the capillary fringe and in streamflow generation.

ACKNOWLEDGEMENTS

This work is part of a PhD research (by the first author), which was funded by the German Academic Exchange Service (DAAD). Field observations were funded by the Water Research Commission (WRC) of South Africa. Technical assistance was received from Mr JJ Pretorius, the chief technician at the School of Engineering and the Centre for Water Resources Research (CWRR), University of KwaZulu-Natal (UKZN). The composition of this paper was initiated during a 3-month stay by the first author at the CWRR (UKZN), under the funding from the Umgeni Water Resources Management, South Africa. The paper was completed from the Department of Disaster Preparedness and Engineering Management (DPEM), Masinde Muliro University of Science and Technology, Kenya. We are very much grateful to the four anonymous reviewers and the handling editor, whose substantial comments greatly helped improve this paper.

REFERENCES

Abdul AS, Gillham RW. 1984. Laboratory studies of the effects of the capillary fringe on streamflow generation. *Water Resources Research* **20**(6): 691–698. DOI:10.1029/WR020i006p00691.

Buttle JM. 1994. Isotope hydrograph separations and rapid delivery of pre-event water from drainage basins. *Progress in Physical Geography* **18**(1): 16–41. DOI:10.1177/030913339401800102.

Buttle JM, Sami K. 1992. Testing the groundwater ridging hypothesis of streamflow generation during snowmelt in a forested catchment. *Journal of Hydrology* **135**(1–4), 53–72. DOI: 10/10.1016/0022-1694(92)90080-F.

Carslaw HS, Jaeger JC. 1959. *Conduction of Heat in Solids*. New York: Oxford University Press, Clarendon Press.

Cloke HL, Anderson MG, McDonnell JJ, Renaud JP. 2006. Using numerical modelling to evaluate the capillary fringe groundwater ridging hypothesis of streamflow generation. *Journal of Hydrology* **316**: 141–162. DOI:10.1016/j.jhydrol.2005.04.017.

Craig H. 1961. Standard for reporting concentrations of deuterium and oxygen-18 in natural waters. *Science* **133**: 1833–1834. DOI:10.1126/science.133.3467.1833.

Dewalle DR, Swistock BR, Sharpe WE. 1988. Three-component tracer model for stormflow on a small Appalachian forested catchment. *Journal of Hydrology* **104**(1–4), 301–310. DOI: 10/10.1016/0022-1694(88)90171-0.

Flury M, Gimmi T. 2002. Solute diffusion. In *Methods of Soil Analysis. Part 4. Physical Methods*. Dane JH, Topp GC (eds). American Society of Agronomy, Madison, Wisconsin, 1323–1351.

Gillham RW. 1984. The capillary fringe and its effect on water-table response. *Journal of Hydrology* **67**(1-4): 307–324. DOI: 10.1016/0022-1694(84)90248-8

Heliotis FD, DeWitt CB. 1987. Rapid water table response to rainfall in a northern peatland ecosystem. *Water Resources Bulletin* **23**(6): 1011–1016. DOI:10.1111/j.1752-1688.1987.tb00850.x.

Horton RE. 1933. The role of infiltration in the hydrologic cycle. *Eos, Transaction American Geophysical Union* **14**: 446–460. DOI:10.1029/TR014i001p00446.

Kennedy VC, Kendall C, Zellweger GW, Wyerman TA, Avanzino RJ. 1986. Determination of the components of stormflow using water chemistry and environmental isotopes, Mattole River Basin, California. *Journal of Hydrology* **84**(1-2): 107–140. DOI: 10/10.1016/0022-1694(86)90047-8.

Kirchner JW. 2003. A double paradox in catchment hydrology and geochemistry. *Hydrological Processes* **17**(4): 871–874. DOI:10.1002/hyp.5108.

Lorentz SA., Thornton-Dibb, S, Hickson, R, Sihlophe, N. 2001. Hydrological systems modelling research programme: hydrological processes. Phase I: processes, definitions and database. WRC Report No. 637/1/01. Water Research Commission, Pretoria, South Africa. 102 pp.

Marino MA. 1974. Rise and decline of the water table induced by vertical recharge. *Journal of Hydrology* **23**(3–4), 289–298. DOI: 10.1016/0022-1694(74)90009-2.

Marui A, Yasuhara M, Kuroda K, Takayama S. 1993. Subsurface water movement and transmission of rainwater pressure through a clay layer. *Proceedings of the Yokohama Symposium, on the Hydrology of Warm Humid Regions, IAHS Publication* No. **216**: 463–470.

Miyazaki T, Khaled IM, Nishiman T. 2012. Shallow groundwater dynamics controlled by the Lisse effect and reverse Wieringermeer effects. *Journal of Sustainable Watershed Science and Management* **1**(2): 36–45. DOI:10.5147/jswsm.2012.0065.

Novakowski KS, Gillham RW. 1988. Field investigations of the nature of water-table response to precipitation in shallow water-table environments. *Journal of Hydrology* **97**(1–2), 23–32. DOI: 10.1016/0022-1694(88)90063-7.

Ogunkoya OO, Jenkins A. 1993. Analysis of storm hydrograph and flow pathways using a three-component hydrograph separation model. *Journal of Hydrology* **142**(1): 71–88. DOI: 10/10.1016/0022-1694(93)90005-T

Rosenberry DO, Winter TC. 1997. Dynamics of water-table fluctuations in an upland between two prairie-pothole wetlands in North Dakota. *Journal of Hydrology* **191**(1): 266–289. DOI:10.1016/S0022-1694(96)03050-8.

Sklash MG, Farvolden RN. 1979. The role of groundwater in storm runoff. *Journal of Hydrology* **43**(1–4): 45–65. DOI: 10/10.1016/S0167-5648(09)70009-7.

Swistock BR, DeWalle DR, Sharpe WE. 1989. Sources of acidic storm flow in an Appalachian headwater stream. *Water Resources Research* **25**(10): 2139–2147. DOI:10.1029/WR025i010p02139.

Waswa GW. 2013. Transient pressure waves in hillslopes. PhD Thesis, School of Engineering, KwaZulu-Natal, Durban, South Africa. 120.

Waswa GW, Lorentz SA. 2015. Transmission of pressure head through the tension saturation zone in the Lisse effect phenomenon. *Hydrological Sciences Journal* http://dx.doi.org/10.1080/02626667.2014.943230.

Waswa GW, Clulow AD, Freese C, le Roux PAL, Lorentz SA. 2013. Transient pressure waves in the vadose zone and the rapid water table response. *Vadose Zone Journal*. DOI:10.2136/vzj2012.0054.

